Septate junction proteins are required for egg elongation and border cell migration during oogenesis in Drosophila

Haifa Alhadyian[*], Dania Shoaib[*], and Robert E. Ward IV[*,1]

[*]Department of Molecular Biosciences, University of Kansas, Lawrence, Kansas 66045

[1]Current address and Corresponding Author information: Robert E. Ward IV, Department of Biology, Case Western Reserve University, 2080 Adelbert Rd, Cleveland, Ohio 44106

E-mail: rew130@case.edu

Phone: (216) 368-6707

Running title: SJ proteins in oogenesis

Keywords: Septate junctions, oogenesis, Drosophila, tissue morphogenesis, egg elongation

Abstract

Protein components of the invertebrate occluding junction - known as the septate junction (SJ) - are required for morphogenetic developmental events during embryogenesis in *Drosophila melanogaster*. In order to determine whether SJ proteins are similarly required for morphogenesis during other developmental stages, we investigated the localization and requirement of four representative SJ proteins during oogenesis: Contactin, Macroglobulin complement-related, Neurexin IV, and Coracle. A number of morphogenetic processes occur during oogenesis, including egg elongation, formation of dorsal appendages, and border cell migration. We found that all four SJ proteins are expressed in egg chambers throughout oogenesis, with the highest and most sustained levels in the follicular epithelium (FE). In the FE, SJ proteins localize along the lateral membrane during early and mid-oogenesis, but become enriched in an apical-lateral domain (the presumptive SJ) by stage 10B. SJ protein relocalization requires the expression of other SJ proteins, as well as Rab5 and Rab11 in a manner similar to SJ biogenesis in the embryo. Knocking down the expression of these SJ proteins in follicle cells throughout oogenesis results in egg elongation defects and abnormal dorsal appendages. Similarly, reducing the expression of SJ genes in the border cell cluster results in border cell migration defects. Together, these results demonstrate an essential requirement for SJ genes in morphogenesis during oogenesis, and suggests that SJ proteins may have conserved functions in epithelial morphogenesis across developmental stages.

Article Summary

Septate junction (SJ) proteins are essential for forming an occluding junction in epithelial tissues in *Drosophila melanogaster*, and also for morphogenetic events that occur prior to the formation of the junction during embryogenesis. Here we show that SJ proteins are expressed in the follicular epithelium of egg chambers during oogenesis and are required for morphogenetic events including egg elongation, dorsal appendages formation, and border cell migration. Additionally, the formation of SJs during oogenesis is similar to that in embryonic epithelia.

Introduction

The septate junction (hereafter referred to as SJ) provides an essential paracellular barrier to epithelial tissues in invertebrate animals (Noirot-timothée *et al.* 1978). As such, the SJ is functionally equivalent to the tight junction in vertebrate tissues, although the molecular components and ultrastructure of these junctions differ (reviewed in Izumi and Furuse 2014). Studies in *Drosophila* have identified more than 20 proteins that are required for the organization or maintenance of the SJ (Fehon *et al.* 1994; Baumgartner *et al.* 1996; Behr *et al.* 2003; Paul *et al.* 2003; Genova and Fehon 2003; Faivre-Sarrailh *et al.* 2004; Wu *et al.* 2004; Wu *et al.* 2007; Tiklová *et al.* 2010; Nelson *et al.* 2010; Ile *et al.* 2012; Bätz *et al.* 2014; Hall *et al.* 2014). Given that some of these genes have clear developmental functions (e.g. *coracle*'s name derives from its dorsal open embryonic phenotype; Fehon *et al.* 1994), we previously undertook an examination of the developmental requirements for a set of core SJ genes (Hall and Ward 2016). We found that all of the genes we analyzed (9 in all) are required for morphogenetic developmental events during embryogenesis including head involution, dorsal closure and salivary gland organogenesis. Interestingly, these embryonic developmental events occur prior to the formation of an intact SJ, suggesting that these proteins have a function independent of their role in creating the occluding junction (Hall and Ward 2016). Since strong loss of function mutations in every SJ gene are embryonic lethal (due to these morphogenetic defects and/or a failure in establishing a blood-brain barrier in glial cells; Baumgartner *et al.* 1996), only a few studies have examined the role of SJ proteins in morphogenesis at a later stages of development. These studies have revealed roles for SJ proteins in planar polarization of the wing imaginal disc, for epithelial rotations in the eye and genital imaginal discs, and ommatidia integrity (Lamb *et al.* 1998; Venema *et al.* 2004; Moyer and Jacobs 2008; Banerjee *et al.* 2008).

To further explore the role of SJ proteins in morphogenesis beyond the embryonic stage, we set out to examine the expression and function of a subset of SJ genes in the *Drosophila* egg chamber during oogenesis. Each of the two *Drosophila* ovaries is comprised of approximately 16-20 ovarioles, which are organized into strings of progressively developing egg chambers (Figure 1A). Each egg chamber forms in a structure called the germarium, where the germline and somatic stem cells reside. Once the egg chamber is formed, it leaves the germarium as a 16-cell germline cyst consisting of 15 nurse cells and an oocyte surrounded by a layer of somatic follicle cells (FCs) (Figure 1B). An egg chamber undergoes 14 developmental stages ending in a mature egg that is ready for fertilization (reviewed in Horne-Badovinac and Bilder 2005). Interfollicular cells called stalk cells connect egg chambers to each other. During oogenesis, the follicular epithelium (FE) participates in several morphogenetic events including border cell migration, dorsal appendage formation and egg elongation (reviewed in Horne-Badovinac and Bilder 2005; Duhart *et al.* 2017).

Previous studies have revealed that a few core components of the SJ are expressed in the ovary, including Macroglobulin complement-related (Mcr), Neurexin IV (Nrx-IV), Contactin (Cont), Neuroglian (Nrg), and Coracle (Cora) (Wei *et al.* 2004; Schneider *et al.* 2006; Maimon *et al.* 2014; Hall *et al.* 2014; Ben-Zvi and Volk 2019), although the developmental expression pattern and subcellular localizations of these proteins had not been thoroughly investigated. Additionally, ultrastructural analysis has revealed the presence of mature SJs in the FE by stage 10/10B of oogenesis (Figure 1C), with incipient SJ structures observed in egg chambers as early as stage 6 (Mahowald 1972; Müller 2000). How SJ maturation occurs in the FE is unknown. In embryonic epithelia, SJ biogenesis is a multistep process in which SJ proteins are initially

localized along the lateral membrane, but become restricted to an apical-lateral region (the SJ) in a process that requires endocytosis and recycling of SJ proteins (Tiklová *et al.* 2010).

Here, we analyzed the expression and subcellular localization of the core SJ proteins Mcr, Cont, Nrx-IV, and Cora throughout oogenesis. We find that all of these SJ proteins are expressed in the FE throughout oogenesis. Interestingly, Mcr, Cont, Nrx-IV, and Cora become enriched at the most apical-lateral region of the membrane in stage 10B/11 egg chambers, coincident with the formation of the SJ revealed by electron microscopy (Mahowald 1972; Müller 2000) . Similar to the biogenesis of SJs in the embryo, this enrichment of SJ proteins to the presumptive SJ requires the function of other SJ genes, as well as *Rab5* and *Rab11*. Functional studies using RNA interference (RNAi) of SJ genes in FCs results in defects in egg elongation, dorsal appendage morphogenesis and border cell migration. Together, these results reveal a strong similarity in the biogenesis of SJ between embryonic and follicular epithelia, demonstrate that at least some components of the SJs are required for morphogenesis in the ovary, and suggest that these roles may be independent of their role in forming an occluding junction.

Material and methods

Fly stocks

All *Drosophila* stocks were maintained on media consisting of corn meal, sugar, yeast, and agar on shelves at room temperature or in incubators maintained at a constant temperature of 25°C. GAL4 lines used in this study are as follows: *GR1-GAL4* (Bloomington Drosophila Stock Center (BDSC) #36287), *Slbo-GAL4, UAS-mCD8-GFP* (BDSC#76363), and *C306-GAL4; GAL80^{ts}/Cyo* (a gift from Jocelyn McDonald, Kansas State University, Manhattan, Kansas). RNAi stocks used

for these studies are as follows: *UAS-Mcr-RNAi* (BDSC#65896 and Vienna Drosophila Resources Center (VDRC)#100197), *UAS-Cora-RNAi* (BDSC#28933 and VDRC#9787), *UAS-Nrx-IV-RNAi* (BDSC#32424 and VDRC#9039), *UAS-Cont-RNAi* (BDSC#28923), *UAS-mCherry-RNAi* (BDSC#35787), *UAS-Lac-RNAi* (BDSC#28940), and *UAS-Sinu-RNAi* (VDRC#44929). *UAS-Rab5*^{DN} (BDSC#9771) was used to inhibit normal Rab5 function and *UAS-Rab11-RNAi* (BDSC#27730) was used to knock down Rab11 in the follicle cells. *UAS-GAL80*^{ts} (BDSC#7108) was used to conditionally inhibit *GR1-GAL4* activity in the *UAS-Rab11-RNAi* experiment. *UAS-GFP* (BDSC#1521) was crossed to *GR1-GAL4* as a control for the egg shape experiments. *Slbo-GAL4, UAS-mCD8-GFP* was crossed to *UAS-mCherry-RNAi* as a control for one set of border cell migration studies, whereas *C306-GAL4; GAL80*^{ts}*/Cyo* was crossed to *UAS-Dcr* (BDSC#24646) as a control for the other set of border cell migration studies. *w*^{1118} (BDSC# 5905) was used as the wild type stock for determining the expression of Mcr, Cont, Nrx-IV and Cora in the follicle cells.

Fly staging

w^{1118} 1-2-day-old females and males were collected and reared at 25^{o}C on fresh food sprinkled with yeast for five to six days before the females were dissection for antibody staining. For egg elongation analyses, crosses were maintained at 25^{o}C, and 1-2-day-old females (control and *UAS-RNAi*-expressing) were mated with sibling males and maintained at 29-30^{o}C for 3 days before dissection. For border cell migration analyses, *Slbo-GAL4* crosses were kept at 25^{o}C, whereas *C306-GAL4/UAS-Dcr; GAL80*^{ts}*/SJ-RNAi* crosses were kept at 18^{o}C to prevent GAL4 activation. 1-2-day-old flies with the appropriate genotype (*Slbo-GAL4, UAS-mCD8-GFP/UAS-RNAi* or *C306-GAL4/UAS-Dcr;UAS-RNAi;GAL80*^{ts}) were shifted to 29-30^{o}C for 48 hours before

dissection. It should be noted that by crossing *UAS-GFP* to *C306-GAL4*, we observed the expression of GFP in polar cells in stage 10, but not stage 9 egg chambers (data not shown). For the *Rab11-RNAi* experiment, crosses were maintained at 18^{o}C and 2-3-day-old males and females with the appropriate genotype (*GR1-GAL4>UAS-mCherry-RNAi, UAS-GAL80ts or GR1-GAL4>UAS-Rab11-RNAi, UAS-GAL80ts*) were collected and reared at 29^{o}C-30^{o}C overnight before dissection. For the *Rab5*^{DN} experiment, crosses were maintained at 25^{o}C, and 1-2-day-old females were mated to sibling males and maintained at 29-30^{o}C for 3 days before dissection.

Egg aspect ratio measurements

Stage 14 egg chambers were selected for analysis based on the overall morphology of the egg and the absence of nurse cells nuclei by DAPI staining. Stage 14 egg chambers that have irregular edges or touch other egg chambers were excluded from the analysis to prevent inaccurate measurements. Egg length (anterior-posterior) and width (dorsal-ventral) were measured using the ImageJ/Fiji (http://fiji.sc) (Schindelin *et al.* 2012) straight-line tool, and aspect ratio was calculated as length divided by width using Microsoft Excel.

Border cell migration quantification

Stage 10 egg chambers were identified based on the morphology of the egg (oocyte occupies half the egg chamber, whereas the other half is occupied by the nurse cells and centripetal cells). We used the GFP signal in *Slbo-GAL4* crosses and DAPI and/or Fas3 staining in *c306-GAL4* crosses to identify the location of the border cell cluster in stage 10 egg chambers. The location of the border cell cluster was quantified and grouped into four categories - complete, incomplete, failed

159 migration, and disassociated cluster based on the location of the cluster relative to the oocyte in a
160 stage 10 egg chamber (Figure 5). In some cases, border cell clusters display two phenotypes such
161 as complete and dissociated. In this case, we quantified both phenotypes in one egg chamber.
162
163 *Immunostaining and image acquisition*
164 Ovaries were dissected in 1X Phosphate-buffered saline (PBS), fixed in 4% Paraformaldehyde
165 for 20 minutes, washed three times in 1X PBS, and then permeabilized in a block solution (1X
166 PBS + 0.1% Triton + 1% Normal Donkey Serum) for 30 minutes before incubation with primary
167 antibodies either overnight at 4^{o}C or 2-4 hours at room temperature. The following antibodies
168 were used at the given dilutions: guinea pig (gp) anti-Cont 1:2000 (Faivre-Sarrailh *et al.* 2004)
169 and rabbit (rab) anti-Nrx-IV 1:500 (Baumgartner *et al*. 1996) obtained from Manzoor Bhat,
170 University of Texas Health Science Center, San Antonio, TX, gp anti-Mcr 1:1000 (Hall *et al*.
171 2014), mouse (m) anti-Cora (C566.9 and C615.16 mixed 1:1, obtained from the Developmental
172 Studies Hybridoma Bank (DSHB) at the University of Iowa, Iowa City, IA; Fehon *et al.* 1994)
173 1:50, rat anti-*D*E-cad (DCAD2, DSHB) 1:27, and m anti-Fas3 (7G10, DSHB) 1:260. DAPI
174 (1mg/ml) was used at a dilution of 1:1000. Cy2-, Cy3-, and Cy5-conjugated secondary
175 antibodies were obtained from Jackson ImmunoResearch Laboratories (West Grove,
176 Pennsylvania, USA) and were used at 1:500.
177 Images were acquired using an Olympus FV1000 confocal microscope equipped with
178 Fluoview software (version 4.0.3.4). Objectives used included an UPLSAPO 20X Oil (NA:0.85),
179 a PLANAPO 60X Oil (NA: 1.42), and an UPLSAPO 100X Oil (NA:1.40). Stage 14 egg
180 chambers were imaged using Nikon Eclipse 80*i* compound microscope. Raw images were
181 rotated and cropped in ImageJ/Fiji. Micrographs were adjusted for brightness using Adobe

Photoshop 21.1.1 (San Jose, CA) or Image/Fiji. Adobe Illustrator 24.1 was used to compile the figures.

Statistical Analysis

An unpaired *t*-test was used to calculate the P values in egg chamber aspect ratio between control and SJ mutant stage 14 egg chambers using GraphPad Prism 8 (https://www.graphpad.com) (version 8.4.2).

Data Availability

Fly stocks are available upon request. Supplemental files are available at FigShare. Figure S1 shows the efficiency of RNAi knock-down in the FE of stage 12 egg chambers. Figure S2 shows the range of dorsal appendage phenotypes found in *GR1>SJ-RNAi* stage 14 egg chambers. Figure S3 shows the expression of Contactin during border cell migration. Figure S4 shows the expression of Nrx-IV during border cell migration. Figure S5 shows the expression of Coracle during border cell migration. Table S1 shows the raw length, width and aspect ratios data for egg shape experiment shown in Figure 3, and the raw data for the border cell migration studies presented in figure 5. The authors affirm that all the data necessary for confirming the conclusions of the article are present within the article, figures and supplemental files.

Results

Septate junction proteins are expressed in follicle cells throughout oogenesis

While a few SJ proteins have previously been reported to be expressed in the *Drosophila* ovary (Wei *et al.* 2004; Schneider *et al.* 2006; Hall *et al.* 2014; Maimon *et al.* 2014; Felix *et al.* 2015; Ben-Zvi and Volk 2019), a thorough analysis of their tissue distribution and subcellular localization throughout oogenesis is lacking. We therefore examined the spatial and temporal expression of four SJ proteins: Mcr, Cont, Nrx-IV and Cora (Fehon *et al.* 1994; Baumgartner *et al.* 1996; Faivre-Sarrailh *et al.* 2004; Bätz *et al.* 2014; Hall *et al.* 2014). These four proteins are core components of the junction for which well-characterized antibodies are available.

At early stages of oogenesis (stages 2-8), Mcr, Cont, and Nrx-IV all localize in puncta at the lateral membrane of FCs and nurse cells, and show a punctate distribution in these cells (Figure 1D-F). Mcr, Cont, and Nrx-IV are also more strongly expressed in polar cells (PCs) than the surrounding FCs (asterisks in Figure 1D-F). Cora is more uniformly localized along the lateral membrane of the FCs, including the PCs (Figure 1G and data not shown). These SJ proteins are additionally expressed in stalk cells (arrowheads in Figure 1 D and E and data not shown). Beginning at stage 10B, Mcr, Nrx-IV, Cont and Cora are gradually enriched at the apical-lateral membrane of the FCs just basal to the AJ. This localization is complete by stage 11 (arrows in Figure 2B, D, F, and H) and persists until the end of oogenesis (Figure 2C, E, G and I). The timing of this apical-lateral enrichment of Mcr, Cont, Nrx-IV and Cora coincides with the maturation of the SJ in the FCs based upon ultrastructural analysis (Mahowald 1972; Müller 2000), and so we will refer to this region as the presumptive SJ.

SJ proteins are required for egg elongation and dorsal appendage morphogenesis

Given our findings that Mcr, Cont, Nrx-IV and Cora are expressed in the FE throughout oogenesis, and our previous studies indicating a role for SJ proteins in morphogenesis, we wondered whether SJ proteins might be required for morphogenetic processes in the FE. The FE plays critical roles in shaping the egg chamber and producing the dorsal appendage, while a subset of FE cells participates in border cell migration to form the micropyle (Montell 2003; Horne-Badovinac 2020). Because SJ mutant animals die during embryogenesis, we used the *GAL4 UAS-RNAi* system to knock-down the expression of SJ proteins in the FCs (Brand and Perrimon 1993). To knock down expression of SJ proteins throughout the majority of oogenesis, we used *GR1-GAL4*, which is expressed in the FCs from stage 4 to 14 of oogenesis (Gupta and Schüpbach 2003; Wittes and Schüpbach 2018). We examined SJ protein expression in late-stage egg chambers for *Mcr-*, *Cora-*, and *Nrx-IV-RNAi* to demonstrate that the RNAi was efficiently knocking down protein expression in this tissue (Figure S1). In all, we tested Bloomington Transgenic RNAi Project (TRiP) lines made against six different SJ genes (*Cont*, *cora*, *Mcr*, *lac*, *Nrx-IV*, and *sinu*). To examine overall egg chamber shape, we dissected stage 14 egg chambers from females expressing *SJ-RNAi* under the control of *GR1-GAL4*, imaged them on a compound microscope, and determined the aspect ratio of the egg chambers using measurements of egg chamber length and width using ImageJ/Fiji. Control stage 14 egg chambers (*GR1-GAL4>UAS-GFP*) had a mean aspect ratio of 2.3 (Figure 3A and J). In contrast, the aspect ratio of stage 14 egg chambers from all *GR1-GAL4>SJ-RNAi* is statistically significantly smaller than the aspect ratio of the control egg chambers (aspect ratios from 1.7 to 2.1, unpaired t-test $P<0.0001$). All *SJ-RNAi* stage 14 egg chambers are also significantly shorter (mean length from 391.9mm to 466mm) than control egg chamber (mean length of 487.6mm) (unpaired *t*-test $P<0.0001$; Figure 3H). Similarly, all (mean of width from 211.8mm to 239.6mm) but *Mcr-RNAi* (BDSC) and *Cont-*

249 *RNAi* are significantly wider than control egg chamber (mean of width 208mm) (unpaired *t*-test
250 $P<0.0001$; Figure 3I). To confirm the specificity of these results we also tested VDRC RNAi
251 lines directed against *Mcr*, *cora*, and *Nrx-IV*, and found similar effects on egg shape (unpaired *t*-
252 test $P<0.0001$; Figure 3). The raw data for all of these analyses can be found in Table S1.
253 Further examination of stage 14 SJ mutant egg chambers revealed defects in dorsal appendage
254 morphology. Dorsal appendages are tubular respiratory structures that form from two
255 populations of the dorsal FE known as floor and roof cells (Duhart *et al.* 2017). The primary
256 phenotypes we observed in the *SJ-RNAi*-expressing egg chambers were missing dorsal
257 appendages, or appendages that appeared to be short or broken (Figures 3L and S2). In addition,
258 nearly all of the *SJ-RNAi*-expressing dorsal appendages that were present appeared to have a
259 thinner stalk than found in control egg chambers (Figure S2). In quantifying these phenotypes,
260 both BDSC and VDRC RNAi lines against *Mcr* (BDSC: 52% , VDRC:18%) and *cora* (BDSC:
261 15% and VDRC: 21%) produced egg chambers with defective dorsal appendages (Fig 3M).
262 Similarly, 19% of *Cont-RNAi*- and 13% of *Lac-RNAi*-expressing egg chambers have either
263 missing or broken dorsal appendages, however the *Nrx-IV-RNAi* BDSC line did not produce
264 abnormal dorsal appendages, whereas 33% of VDRC *Nrx-IV-RNAi* line resulted in defective
265 dorsal appendages. We also did not observe defective dorsal appendages in *Sinu-RNAi*-
266 expressing egg chambers (Figure 3M).
267
268 *SJ proteins are expressed in polar and border cells and are required for effective border cell*
269 *migration*
270 The observation that Mcr, Cont, and Nrx-IV are strongly expressed in PCs and in all FCs
271 (Figure 1D-F), motivated us to investigate their expression during the process of border cell

migration. Border cell migration occurs during stages 9-10 of oogenesis (Figure 4A). During stage 9, signaling from the anterior PCs recruits a group of 4-8 adjacent FCs to form a cluster and delaminate apically into the egg chamber. The border cell cluster is organized with a pair of PCs in the center surrounded by border cells. This cluster of cells migrates between the nurse cells until they reach the anterior side of the oocyte (Figure 4A). This process takes approximately 4-6 hours and is complete in wild type egg chambers by stage 10 of oogenesis (Prasad and Montell 2007). The border cell cluster, along with the migratory centripetal cells, collaborate to form the micropyle, a hole through which the sperm enters the egg (Figure 4A) (Montell 2003; Horne-Badovinac 2020). Previous studies showed that Cora and Nrg are expressed in the PCs during their migration (Wei *et al.* 2004; Felix *et al.* 2015). To determine if other SJ proteins are also expressed during border cell migration, we stained stage 9-10 wild type egg chambers with antibodies against Mcr, Cont, Nrx-IV and Cora. To mark the PCs, we co-stained the egg chambers with Fasciclin 3 (Fas3; Snow *et al.* 1989; Khammari *et al.* 2011). Mcr, Cont, Nrx-IV and Cora are all expressed in border cell clusters throughout their migration (Figure 4B-D and S3-5). Interestingly, the expression of these SJ proteins in PCs appears highest at the interfaces between polar and border cells (Figure 4B-D and Figures S3-5). SJ protein expression is also asymmetric in the border cell cluster, with higher expression along border cells closest to the oocyte, raising the possibility that these proteins may respond to or direct leading-edge polarity in the migrating border cell cluster (red arrows in Figure 4B-D).

Given that Mcr, Cont, Nrx-IV and Cora are expressed in border cell clusters throughout border cell migration, we wondered if they are also required for some aspect of this process. To address this issue, we used *Slbo-GAL4* (Ogienko *et al.* 2018) to express RNAi against individual SJ genes specifically in border cells and analyzed the border cell clusters at stage 10 in these

ovaries. We noticed a range of defective migration phenotypes in these egg chambers and classified them into three non-exclusive groups: failed, incomplete and dissociated clusters. Complete migration (Figure 5A-C) is characterized by having the entire border cell cluster physically touching or just adjacent the oocyte by the end of stage 10 (Figure 5C). A failed cluster is characterized by a border cell cluster that has not delaminated from the FE by stage 10 (Figure 5D). An incomplete migration phenotype is characterized as an intact cluster that has not reached the oocyte by the end of stage 10 (Figure 5E, where the two dashed lines indicate the range of distances at which border cell clusters were categorized as incomplete). Finally, a dissociated cluster phenotype is characterized by a cluster that has broken into a linear string of border cells or that has one or more border cells that remain between nurse cells and are not connected to the larger border cell cluster (Figure 5F and H).

In control stage 10 egg chambers (*Slbo-GAL4; UAS-mCD8-GFP/UAS-mCherry-RNAi*), 86% (n=81) of border cell clusters completed their migration, with the remainder showing incomplete migration (Figure 5I). In contrast, stage 10 egg chambers expressing RNAi against *cora*, *Nrx-IV,* or *Cont* in the border cells resulted in 58% (n=67), 50% (n=74), and 40% (n=85) of border cell clusters completing migration, respectively (Figure 5I). The remaining *cora-RNAi-* and *Nrx-IV-RNAi*-border cell clusters showed a combination of incomplete migration or failed to delaminate (Figure 5I). *Cont-RNAi*-border cell clusters also showed 35% of incomplete border cell migration, but additionally had 17% of the clusters disassociating during their migration (Figure 5E, F, H and I). *Mcr-RNAi*-border cell clusters were indistinguishable from controls with 86% (n=94) completing their migration and the remainder showing only 13% incomplete migration (Figure 5I).

To extend these studies, we examined border cell migration in egg chambers expressing RNAi against SJ genes using the *C306-GAL4* driver. *C306-GAL4* is expressed in the border cells throughout the process of border cell migration (Murphy and Montell 1996) and in PCs just at stage 10 (H.A., unpublished observation). In control egg chambers (*C306-GAL4/UAS-Dcr; $GAL80^{ts}$/+), 78% (n=91) of BC clusters completed their migration and 19% displayed incomplete migration (Figure 5J). Stage 10 egg chambers expressing *C306>Mcr-RNAi* displayed 66% (n=98) complete border cell migration with 30% showing incomplete migration, 5% showing dissociated clusters and 3% showing failed border cell migration (Figure 5J). Similarly, egg chambers expressing *C306>Nrx-IV-RNAi* displayed 66% (n=59) complete border cell migration with 30% showing incomplete migration and 3% failing to delaminate (Figure 5J). Finally, 78% (n=70) of stage 10 *C306>cora-RNAi*-expressing border cells displayed complete border cell migration, whereas 20% showed incomplete migration and 3% failed to delaminate (Figure 5J).

SJ biogenesis in the follicular epithelium

The redistribution of SJ proteins in the FCs of later stage egg chambers resembles the dynamic relocalization of SJ proteins during the biogenesis of the junction during embryogenesis (Tiklová *et al.* 2010). In embryonic epithelia, SJ protein enrichment at the apical-lateral domain (presumptive SJ) requires endocytosis and recycling of SJ proteins to the membrane, and is interdependent on the presence of all core SJ proteins (Ward *et al.* 1998; Hall *et al.* 2014). Coincident with the strong localization of SJ proteins to the presumptive SJ at stage 16 of embryogenesis, ladder-like electron-dense intermembrane septa are visible by electron microscopy that become progressively organized by stage 17 (Schulte *et al.* 2003; Hildebrandt *et*

339 *al.* 2015). We therefore sought to determine if similar processes occur during the formation of
340 SJs in the FE.

341 To test for the interdependence of SJ proteins for localization, we examined Cora and Mcr
342 expression in wild type, *Mcr-RNAi*, and *Nrx-IV-RNAi* stage 12 FCs. In wild type stage 12 egg
343 chambers, Cora is strongly co-localized with Mcr at the apical-lateral domain of the FCs
344 (completely penetrant in 95 cells from 31 egg chambers) (Figure 6A). In contrast, Cora and Mcr
345 are mislocalized along the lateral domain in stage 12 *Nrx-IV-RNAi* FCs (Figure 6B), much like
346 they are in stage 2-8 wild type FCs (Figure 1D). Specifically, 6 out of 20 *Nrx-IV-RNAi* FCs cells
347 from 19 egg chambers showed complete mislocalization, whereas 13 of these 20 cells showed
348 largely lateral localization with some degree of apical enrichment. Similarly, in stage 12 *Mcr-*
349 *RNAi* FCs, Cora was mislocalized along the lateral membrane in 39 out of 47 cells examined
350 from 19 egg chambers, with the remaining 8 cells showing some enrichment of Cora at the apical
351 lateral domain (Figure 6C). Notably, cells that showed apical enrichment of Cora also retained
352 small foci of Mcr expression that overlaps with the enriched Cora (Figure 6D), suggesting the
353 perdurance of Mcr in these cells may have allowed for normal SJ organization. Together, these
354 experiments indicate that SJ biogenesis in the FE of late-stage egg chambers requires the
355 expression of at least some core SJ proteins.

356 We next wanted to investigate whether the relocalization of SJ proteins to the presumptive SJ
357 required endocytosis and recycling. In the embryonic hindgut, Cora, Gliotactin (Gli), Sinu, and
358 Melanotransferrin (Mtf) localize with the early endosomal marker, Rab5, and partially localize
359 with the recycling marker, Rab11 during SJ biogenesis (Tiklová *et al.* 2010). Moreover, blocking
360 Rab5 or Rab11 function prevents Cora, Gli, Sinu, and Mtf apical-lateral localization *(Tiklová et*
361 *al*. 2010), and thus SJ formation. To determine if similar processes occur during SJ formation in

FCs, we expressed a dominant negative version of Rab5 (*UAS-Rab5^{DN}*) in FCs using *GR1-GAL4* and examined the expression of Mcr and Cora in stage 11 FCs. In wild-type FCs at that stage, Mcr and Cora are enriched at the apical-lateral membrane (completely penetrant in 91 cells from 15 egg chambers; arrows in Figure 7A), whereas both Mcr and Cora remains localized along the lateral membrane in the Rab5^{DN}-expressing FCs (n=97 cells, 15 egg chambers; Figure 7B). Similarly, Cora and Mcr co-localize at the apical-lateral membrane of the FCs of stage 12 egg chambers (n=64 cells, 15 egg chambers; arrows in Figure 7C), whereas knocking down the expression of Rab11 in stage 12 FCs (via *GR1>Rab11-RNAi*) resulted in the mislocalization of Cora and Mcr (n=23 cells out of 44, 16 egg chambers; arrow in Figure 7D). Cora is exclusively mislocalized along the lateral membrane in these cells, whereas Mcr is most frequently missing from the plasma membrane, either in punctate cytoplasmic foci or completely gone (in 21 of the 23 *Rab11-RNAi* cells; Figure 7D). Interestingly, we noted that the FE in *Rab5^{DN}*- and *Rab11-RNAi*-expressing egg chambers are taller in the apical/basal dimension than similarly staged wild type egg chambers (compare Figure 7A with 7B and Figure 7C with 7D), although the effect is greater with *Rab5^{DN}* than with *Rab11-RNAi*. Taken together, these results indicate that similar to embryonic epithelia, the maturation of SJs in the FE requires Rab5-mediated endocytosis and Rab11-mediated recycling.

Discussion

In this study, we have demonstrated that a subset of SJ proteins is expressed in egg chambers throughout oogenesis and are required for critical morphogenetic processes that shape the egg, including egg chamber elongation, dorsal appendage formation and border cell migration.

385 Interestingly, the subcellular localization of these SJ proteins in the ovarian FCs changes
386 coincident with the establishment of the occluding junction in much the same way that they do
387 during embryogenesis in ectodermal epithelial cells (Tiklová *et al.* 2010), suggesting that a
388 similar maturation process for the SJ occurs in this tissue.
389
390 *Biogenesis of the SJ in the FE*
391 The mechanisms of SJ biogenesis in embryonic epithelia has been well-studied and involves
392 several steps in which transmembrane SJ proteins are first localized all along lateral plasma
393 membranes (by stage 12 of embryogenesis), but then must be endocytosed and recycled back to
394 the plasma membrane prior to aggregating in the region of the presumptive SJ (between stages
395 13 and 16; Tiklová *et al.* 2010). Prior to this relocalization step, SJ proteins show high mobility
396 in the plane of the membrane by Fluorescence Recovery After Photobleaching (FRAP) analysis,
397 but become strongly immobile as the relocalization is occurring (Oshima and Fehon 2011). As
398 these steps are occurring (e.g. stage 14 of embryogenesis), electron-dense material begins to
399 accumulate between adjacent cells in the presumptive SJ that takes on the appearance of ladder-
400 like septa by stage 17 of embryogenesis (Tepass and Hartenstein 1994). Functional studies
401 indicate that the occluding function of the junction is established late in embryogenesis, near the
402 end of stage 15 (Paul *et al.* 2003). Importantly, the process of SJ biogenesis is interdependent on
403 the function of all core components of the junction and several accessory proteins including Rab
404 5 and Rab 11 (Ward *et al.* 1998; Genova and Fehon 2003; Tiklová *et al.* 2010).
405 Here, we observe that many of these same steps occur in the maturation of SJs in the FE. We
406 first show that SJ proteins are expressed in the FE beginning early in ovarian development where
407 they localize all along the lateral membrane (Figure 1). These proteins appear to become

enriched at the presumptive SJ by stage 11 (Figure 6). The relocalization of SJ proteins to the SJ requires core SJ proteins including Mcr and Nrx-IV, and accessory proteins including Rab 5 and Rab 11 (Figures 6 and 7). Prior studies indicate the presence of electron dense material between FE cells as early as stage 6 (Müller 2000), with a ladder-like appearance of extracellular septa by stage 10B (Mahowald 1972). A recent study of the occluding function in the FE show a similar pattern of protein localization for endogenously tagged Neuroglian-YFP and Lachesin-GFP, and demonstrates that an intact occluding junction is formed during stage 11 of oogenesis (Isasti-Sanchez *et al.* 2020). It is interesting to note the FE is a secondary epithelium initiated by a mesenchymal to epithelial transition (Tepass *et al.* 2001), and yet SJ biogenesis appears to be very similar to that observed in the primary epithelia found in the embryo.

SJ proteins are required for morphogenetic events during oogenesis

The similarities in the dynamic expression of SJ proteins in the FE and embryonic epithelia, coupled with the observation that SJ proteins are required for numerous embryonic developmental events (Hall *et al.* 2014) and references therein) motivated us to explore whether SJ proteins have similar roles in morphogenetic processes that shape the egg. Using a targeted RNAi approach, we show that reducing the expression of *Mcr*, *Nrx-IV*, *Cont*, *cora*, *sinu*, or *lac* throughout oogenesis in the FCs results in significantly rounder stage 14 egg chambers, with many showing additional defects in dorsal appendages (Figures 3 and S2). The initiation and maintenance of egg elongation is achieved at various stages throughout oogenesis (Gates 2012; Bilder and Haigo 2012; Cetera and Horne-Badovinac 2015). From stage 3-6, a gradient of JAK-STAT signaling is required at each pole of the egg chamber to promote Myosin II-based apical cell contractions (Alégot *et al.* 2018). From stage 6-8, collective FC rotation over the germline

generates a robust planar polarized molecular corset consisting of basement membrane protein fibrils aligned with the basal actin cytoskeleton that is required for egg elongation (Gutzeit *et al.* 1991; Frydman and Spradling 2001; Bateman *et al.* 2001; Viktorinová *et al.* 2009; Haigo and Bilder 2011; Horne-Badovinac *et al.* 2012; Cetera *et al.* 2014; Isabella and Horne-Badovinac 2016; Campos *et al.* 2020). During the middle stages of oogenesis (stages 9 and 10), basal actin stress fibers undergo actomyosin contractions, which contribute to egg elongation (He *et al.* 2010; Qin *et al.* 2017). Finally, later in oogenesis, the maintenance of a planar polarized molecular corset is required to retain an elongated egg chamber shape (Haigo and Bilder 2011; Cha *et al.* 2017; Campos *et al.* 2020). Future studies are needed to determine how SJ proteins participate in these events to establish and/or maintain egg shape. Since many of the events involved in egg elongation occur prior to the formation of the occluding junction in the FE, it raises the possibility that much like during embryogenesis, SJ proteins may have a function in morphogenesis that is independent of their role in forming a tight occluding junction.

Stage 14 egg chambers from many of the *SJ-RNAi* lines possessed aberrant dorsal appendages, often characterized by misshapen, broken or missing appendages (Figures 3 and S2). The formation of dorsal appendages occurs during stages 10B-14 and requires cell shape changes and cell rearrangements, coupled with chorion protein secretion (Dorman *et al.* 2004). Similar morphogenetic processes are required for dorsal closure and head involution during embryogenesis (Hayes and Solon 2017; VanHook and Letsou 2008), defects strongly associated with zygotic loss of SJ expression in the embryo (Hall and Ward 2016). We are interested to determine if the mechanism by which SJ proteins contribute to dorsal appendages formation and dorsal closure and head involution are similar. Potential roles could involve regulating the cytoskeleton to facilitate cell shape changes and rearrangements. These observations also suggest

454 the possibility that SJ proteins may be required for chorion protein secretion or crosslinking.
455 Broken and missing dorsal appendages may result from mechanical disruption due to chorion
456 defects. We also noticed mature *SJ-RNAi* eggs with a thin chorion (data not shown). Notably,
457 embryos with mutations in several different SJ genes show defects in the embryonic cuticle
458 including faint denticle belts and delamination of cuticle layers (Lamb *et al.* 1998; (Hall and
459 Ward 2016).

460 Our observation that specifically knocking down the expression of several SJ proteins in
461 border cells results in defective border cell migration (Figure 5) supports a role for SJ proteins in
462 morphogenesis, independent of their role in forming an occluding junction. The phenotypes we
463 observed include failing to complete migration and partial disassociation of the complex by the
464 end of stage 10, which is prior to the formation of an intact SJ. Although the penetrance of these
465 phenotypes is mild (Figure 5I and J), it is possible that these phenotypes underestimate the full
466 requirement of SJ proteins in border cell migration since this process takes a relatively short time
467 (4-6 hours) (Prasad and Montell 2007), while SJ proteins are thought to be very stable in the
468 membrane (Oshima and Fehon 2011). One caveat to the idea that perdurance may account for the
469 mild phenotypes is that *C306-GAL4* does not appear to produce a stronger phenotype than *slbo-*
470 *GAL4*, even though it is expressed earlier and is presumably knocking down SJ proteins longer.
471 Perhaps knocking the proteins down more quickly using the DeGradFP system (Caussinus,
472 Kanca, and Affolter 2012) could address this possibility in the future. These phenotypes also
473 indicate a potential role for SJ proteins in cell adhesion and/or cell polarity during migration.
474 Specifically, we note that Mcr appears to be enriched in polar cell membranes that contact border
475 cells at the leading edge of the cluster (those that are oriented closest to the oocyte) in wild type
476 egg chambers (Figure 4). Whether SJ proteins are required for aspects of planar polarity in the

border cell cluster is an interesting unanswered question. Perhaps the incomplete migration defect results from a meandering migration through the nurse cells, something that has been observed for knockdown of DE-Cadherin in border cells (Cai *et al.* 2014). Live imaging studies should be able to distinguish between pathfinding defects and a general reduction in speed or premature stopping. A role for SJ proteins in cell adhesion in the ovary has been reported previously. Reducing the level of Nrg in FCs results in the failure of FCs that are born outside of the FE due to misoriented spindles to reintegrate into the FE, indicating a role for *Nrg* in lateral cell adhesion (Bergstralh *et al.* 2015). Similarly, expressing a null allele of *Nrg* in FCs enhances the invasive tumor phenotype of a *Discs Large* (*Dlg*) mutation (Wei *et al.* 2004).

Acknowledgements

We thank Jocelyn McDonald, the Bloomington *Drosophila* Stock Center, and the Vienna *Drosophila* RNAi Center for fly stocks. We thank Manzoor Bhat and the Developmental Studies Hybridoma Bank (created by the NICHD of the NIH and maintained at The University of Iowa, Department of Biology, Iowa City, IA 52242) for antibodies used in this study. We thank Brian Ackley for the use of his Olympus FV1000 confocal microscope. We thank Lindsay Ussher for preliminary studies on border cell migration and thoughtful discussions on the project. We also thank Sally Horne-Badovinac, Jocelyn McDonald, Yujun Chen, and members of the Ward lab for helpful discussion about the project and manuscript.

References:

Alégot, H., P. Pouchin, O. Bardot, and V. Mirouse, 2018 Jak-Stat pathway induces *Drosophila* follicle elongation by a gradient of apical contractility. ELife. 7: 1–21.

Banerjee, S, R. J. Bainton, N. Mayer, R Beckstead, and M. A. Bhat, 2008 Septate junctions are required for ommatidial integrity and blood-eye barrier function in *Drosophila*. Dev. Biol. 317: 585–99.

Bateman, J., R. S. Reddy, H. Saito, and D. Van Vactor, 2001 The receptor tyrosine phosphatase dlar and integrins organize actin filaments in the *Drosophila* follicular epithelium. Curr. Biol. 11: 1317–1327.

Bätz, T., D. Förster, and S. Luschnig, 2014 The transmembrane protein macroglobulin complement-related is essential for septate junction formation and epithelial barrier function in *Drosophila*. Development. 141: 899–908.

Baumgartner, S., J. T. Littleton, K. Broadie, M. A. Bhat, R. Harbecke *et al.,* 1996 A *Drosophila* neurexin is required for septate junction and blood-nerve barrier formation and function. Cell. 87: 1059–1068.

Behr, M., D. Riedel, and R. Schuh, 2003 The claudin-like megatrachea is essential in septate junctions for the epithelial barrier function in *Drosophila*. Dev. Cell. 5: 611–620.

Ben-Zvi, D. S., and T. Volk, 2019 Escort cell encapsulation of *Drosophila* germline cells is maintained by irre cell recognition module proteins. Bio. Open. 8.

Bilder, D., and S. L. Haigo, 2012 Expanding the morphogenetic repertoire: perspectives from the *Drosophila* egg. Dev. Cell. 22: 12–23.

Brand, A. H., and N. Perrimon, 1993 Targeted gene expression as a means of altering cell fates and generating dominant phenotypes. Development. 118: 401–415.

519 Cai, D., S. C. Chen, M. Prasad, L. He, X. Wang *et al.,* 2014 Mechanical feedback through E-
520 cadherin promotes direction sensing during collective cell migration. Cell. 157: 1146–1159.
521 Campos, F. C., C. Dennis, H. Alégot, C. Fritsch, A. Isabella *et al.,* 2020 Oriented basement
522 membrane fibrils provide a memory for F-actin planar polarization via the dystrophin-
523 dystroglycan complex during tissue elongation. Development. 147.
524 Caussinus, E., O. Kanca, and M. Affolter, 2012 Fluorescent fusion protein knockout mediated by
525 anti-GFP nanobody. Nat. Struct. and Mol. Biol. 19: 117–121.
526 Cetera, M., and S. Horne-Badovinac, 2015 Round and round gets you somewhere: collective cell
527 migration and planar polarity in elongating *Drosophila* egg chambers. Curr. Opin. Genet.
528 Dev. 32: 10–15.
529 Cetera, M., G. R. Ramirez-San Juan, P. W. Oakes, L. Lewellyn, M. J. Fairchild *et al.,* 2014
530 Epithelial rotation promotes the global alignment of contractile actin bundles during
531 *Drosophila* egg chamber elongation. Nat. Commun. 5:5511.
532 Cha, I. J., J. H. Lee, K. S. Cho, and S. B. Lee, 2017 Drosophila tensin plays an essential role in
533 cell migration and planar polarity formation during oogenesis by mediating integrin-
534 dependent extracellular signals to actin organization. Biochem. Biophys. Res. Commun.
535 484: 702–709.
536 Dorman, J. B., K. E. James, S. E. Fraser, D. P. Kiehart, and C. A. Berg, 2004 Bullwinkle is
537 required for epithelial morphogenesis during *Drosophila* oogenesis. Dev. Biol. 267: 320–
538 341.
539 Duhart, J. C., T. T. Parsons, and L. A. Raftery, 2017 The repertoire of epithelial morphogenesis
540 on display: progressive elaboration of *Drosophila* egg structure. Mech. Dev. 148: 18-39.
541 Faivre-Sarrailh, C., S. Banerjee, J. Li, M. Hortsch, L. Monique, and M. A. Bhat, 2004

Drosophila contactin, a homolog of vertebrate contactin, is required for septate junction organization and paracellular barrier function. Development. 131: 4931–4942.

Fehon, R. G., I. A. Dawson, and S. Artavanis-Tsakonas, 1994 A *Drosophila* homologue of membrane-skeleton protein 4.1 is associated with septate junctions and is encoded by the coracle gene. Development. 120: 545–557.

Felix, M., M. Chayengia, R. Ghosh, A. Sharma, and M. Prasad, 2015 Pak3 regulates apical-basal polarity in migrating border cells during *Drosophila* oogenesis. Development. 142: 3692–3703.

Frydman, H. M., and A. C. Spradling, 2001 The receptor-like tyrosine phosphatase lar is required for epithelial planar polarity and for axis determination within *Drosophila* ovarian follicles. Development. 128: 3209–3220.

Gates, J, 2012 *Drosophila* egg chamber elongation: insights into how tissues and organs are shaped. Fly. 6: 213–227.

Genova, J. L., and R. G. Fehon, 2003 Neuroglian, gliotactin, and the Na+/K+ ATPase are essential for septate junction function in *Drosophila*. J. Cell Biol. 161: 979–989.

Gupta, T., and T. Schüpbach, 2003 Cct1, a phosphatidylcholine biosynthesis enzyme, is required for *Drosophila* oogenesis and ovarian morphogenesis. Development. 130: 6075–6087.

Gutzeit, H. O., and W. Eberhardt, 1991 Laminin and basement membrane-associated microfilaments in wild-type and mutant *Drosophila* ovarian follicles. J. Cell Sci. 100: 781–788.

Haigo, S. L., and D. Bilder, 2011 Global tissue revolutions in a morphogenetic movement controlling elongation. Science 331: 1071–1074.

Hall, S., C. Bone, K. Oshima, L. Zhang, M. McGraw *et al.,* 2014 Macroglobulin complement-

related encodes a protein required for septate junction organization and paracellular barrier function in *Drosophila*. Development. 141: 889–898.

Hall, S., and R. E. Ward, 2016 Septate junction proteins play essential roles in morphogenesis throughout embryonic development in *Drosophila*. G3. 6: 2375–2384.

Hayes, P., and J. Solon, 2017 *Drosophila* dorsal closure: an orchestra of forces to zip shut the embryo. Mech. Dev. 144: 2–10.

He, L., X. Wang, H. L. Tang, and D. J. Montell, 2010 Tissue elongation requires oscillating contractions of a basal actomyosin network. Nat. Cell Biol. 12: 1133–1142.

Hildebrandt, A., R. Pflanz, M. Behr, T. Tarp, D. Riedel *et al.,* 2015 Bark beetle controls epithelial morphogenesis by septate junction maturation in *Drosophila*. Dev. Biol. 400: 237–247.

Horne-Badovinac, S., 2020 The *Drosophila* micropyle as a system to study how epithelia build complex extracellular structures. Philos. Trans. R. Soc. Lond. B Biol. Sci. 375: 20190561.

Horne-Badovinac, S., and D. Bilder, 2005 Mass transit: epithelial morphogenesis in the *Drosophila* egg chamber. Dev. Dyn. 232: 559–574.

Horne-Badovinac, S., J. Hill, G. Gerlach, W. Menegas, and D. Bilder, 2012 A screen for round egg mutants in *Drosophila* identifies tricornered, furry, and misshapen as regulators of egg chamber elongation. G3. 2: 371–378.

Ile, K. E., R. Tripathy, V. Goldfinger, and A. D. Renault, 2012 Wunen, a *Drosophila* lipid phosphate phosphatase, is required for septate junction-mediated barrier function. Development. 139: 2535–2546.

Isabella, A. J., and S. Horne-Badovinac, 2016 Rab10-mediated secretion synergizes with tissue movement to build a polarized basement membrane architecture for organ morphogenesis.

589 Dev. Biol. 38: 47–60.
590 Isasti-Sanchez, J., F. Munz-Zeise, and S. Luschnig, 2020 Transient opening of tricellular vertices
591 controls paracellular transport through the follicle epithelium during *Drosophila* oogenesis.
592 BioRxiv 2020.02.29.971168.
593 Izumi, Y., and M. Furuse, 2014 Molecular organization and function of invertebrate occluding
594 junctions. Semin. Cell Dev. Biol. 36: 186–193.
595 Khammari, A., F. Agnès, P. Gandille, and A. M. Pret, 2011 Physiological apoptosis of polar cells
596 during *Drosophila* oogenesis is mediated by hid-dependent regulation of Diap1. Cell Death
597 and Differ. 18: 793–805.
598 Lamb, R. S., R. E. Ward, L. Schweizer, and R. G. Fehon, 1998 Drosophila coracle, a member of
599 the protein 4.1 superfamily, has essential structural functions in the septate junctions and
600 developmental functions in embryonic and adult epithelial cells. Mol. Biol. Cell. 9: 3505–
601 3519.
602 Mahowald, A. P, 1972 Ultrastructural observations on oogenesis in *Drosophila*. J. Morphol. 137:
603 29–48.
604 Maimon, I., M. Popliker, and L. Gilboa, 2014 Without children is required for Stat-mediated
605 Zfh1 transcription and for germline stem cell differentiation. Development. 141: 2602–
606 2610.
607 Montell, D. J, 2003 Border-cell migration: the race is on. Nat. Rev. Mol. Cell Biol. 4: 13–24.
608 Moyer, K. E., and J. R. Jacobs, 2008 Varicose: a MAGUK required for the maturation and
609 function of *Drosophila* septate junctions. Dev. Dyn. 8: 52–67.
610 Müller, H. J, 2000 Genetic control of epithelial cell polarity: lessons from *Drosophila*. Dev. Dyn.
611 218: 52–67.

612 Murphy, A. M., and D. J. Montell, 1996 Cell type-specific roles for Cdc42, Rac, and Rhol in
613 *Drosophila* oogenesis. J. Cell Biol. 133: 617–630.
614 Nelson, K. S., M. Furuse, and G.J. Beitel, 2010 The *Drosophila* claudin kune-kune is required
615 for septate junction organization and tracheal tube size control. Genetics. 185: 831–839.
616 Noirot-timothée, C., D. S. Smith, M. L. Cayer, and C. Noirot, 1978 Septate junctions in insects:
617 comparison between intercellular and intramembranous structures. Tissue Cell. 10: 125–
618 136.
619 Ogienko, A. A., L. A. Yarinich, E. V. Fedorova, M. O. Lebedev, E. N. Andreyeva *et al.,* 2018
620 New Slbo-Gal4 driver lines for the analysis of border cell migration during *Drosophila*
621 oogenesis. Chromosoma. 127: 475–487.
622 Oshima, K. and R. G. Fehon, 2011 Analysis of protein dynamics within the septate junction
623 reveals a highly stable core protein complex that does not include the basolateral polarity
624 protein discs large. J. Cell Sci. 124: 2861–2871.
625 Paul, S. M., M. Ternrt, P. Salvaterra, and G. Beitel, 2003 The Na+/K+ ATPase is required for
626 septate junction function and epithelial tube-size control in the *Drosophila* tracheal system.
627 Development. 130: 4963–4974.
628 Prasad, M., and D. J. Montell, 2007 Cellular and molecular mechanisms of border cell migration
629 analyzed using time-lapse live-cell imaging. Dev. Cell. 12: 997–1005.
630 Qin, X., B. O. Park, J. Liu, B. Chen, V. Choesmel-Cadamuro *et al.,* 2017 Cell-matrix adhesion
631 and cell-cell adhesion differentially control basal myosin oscillation and *Drosophila* egg
632 chamber elongation. Nat. Commun. 8.
633 Schindelin, J., I. Arganda-Carreras, E. Frise, V. Kaynig, M. Longair *et al.,* 2012 Fiji: an open-
634 source platform for biological-image analysis. Nat. Methods. 9: 676–682.

635 Schneider, M., A.K. Khalil, J. Poulton, C. Castillejo-Lopez, D. Egger-Adam *et al.,* 2006
636 Perlecan and dystroglycan act at the basal side of the *Drosophila* follicular epithelium to
637 maintain epithelial organization. Development. 133: 3805–3815.
638 Schulte, J., U. Tepass, and V. J. Auld, 2003 Gliotactin, a novel marker of tricellular junctions, is
639 necessary for septate junction development in *Drosophila*. J. Cell Biol. 161: 991–1000.
640 Snow, P. M., A. J. Bieber, and C. S. Goodman, 1989 Fasciclin III: a novel homophilic adhesion
641 molecule in *Drosophila*. Cell. 59: 313–323.
642 Spradling, A. C., M. De Cuevas, D. Drummond-Barbosa, L. Keyes, M. Lilly *et al.,* 1997 The
643 *Drosophila* germarium: stem cells, germ line cysts, and oocytes. Cold Spring Harbor Symp.
644 Quant. Biol. 62: 25–34.
645 Tepass, U., and V. Hartenstein, 1994 The development of cellular junctions in the *Drosophila*
646 embryo. Dev. Biol. 161: 563-596.
647 Tepass, U., G. Tanentzapf, R. Ward, and R. Fehon, 2001 Epithelial cell polarity and cell
648 junctions in *Drosophila*. Annu. Rev. Genet. 35: 747–784.
649 Tiklová, K., K. A. Senti, S. Wang, A. GräCurrency Signslund, and C. Samakovlis, 2010
650 Epithelial septate junction assembly relies on melanotransferrin iron binding and
651 endocytosis in *Drosophila*. Nat. Cell Biol. 12: 1071–1077.
652 VanHook, A., and A. Letsou, 2008 Head involution in *Drosophila*: genetic and morphogenetic
653 connections to dorsal closure. Dev. Dyn. 237: 28–38.
654 Venema, D. R., T. Zeev-Ben-Mordehai, and V. J. Auldi, 2004 Transient apical polarization of
655 gliotactin and coracle is required for parallel alignment of wing hairs in *Drosophila*. Dev.
656 Biol. 275: 301–314.
657 Viktorinová, I., T. König, K. Schlichting, and C. Dahmann, 2009 The cadherin Fat2 is required

for planar cell polarity in the *Drosophila* ovary. Development. 136: 4123–4132.

Ward, R. E., R. S. Lamb, and R. G. Fehon, 1998 A conserved functional domain of Drosophila coracle is required for localization at the septate junction and has membrane-organizing activity. J. Cell Biol. 140: 1463–1473.

Wei, J., M. Hortsch, and S. Goode, 2004 Neuroglian stabilizes epithelial structure during *Drosophila* oogenesis. Dev. Dyn. 230: 800–808.

Wittes, J., and T. Schüpbach, 2018 A gene expression screen in *Drosophila melanogaster* identifies novel JAK/STAT and EGFR targets during oogenesis. G3. 9: 47–60.

Wu, V. M., J. Schulte, A. Hirschi, U. Tepass, and G.J. Beitel, 2004 Sinuous is a *Drosophila* claudin required for septate junction organization and epithelial tube size control. J. Cell Biol. 164: 313–323.

Wu, V. M., M. H. Yu, R. Paik, S. Banerjee, Z. Liang *et al.,* 2007 *Drosophila* varicose, a member of a new subgroup of basolateral MAGUKs, is required for septate junctions and tracheal morphogenesis. Development. 134: 999–1009.

Figure Legends

Figure 1. Mcr, Cont, Nrx-IV, and Cora expression during early stages of oogenesis. (A) Diagram of a female *Drosophila* ovariole. Egg chambers are formed in the most anterior region of the ovariole called the germarium (Germ). Each egg chamber undergoes 14 developmental stages while connected to each other through stalk cells (SCs) to form a mature stage 14 egg. (B) Diagram of a stage 8 egg chamber. The egg chamber consists of 15 nurse cells (NCs) and one

oocyte (Oo.), which are surrounded by a monolayer of follicle cells (FCs). At the anterior and posterior ends of an egg chamber resides a pair of differentiated FCs called polar cells (PCs). (C) Diagram of a lateral view of a portion of a stage 10B egg chamber. FCs face the germline and have defined apical-basal polarity with the apical surface facing the germline and a lateral junctional complex consisting of a marginal zone (MZ), an adherens junction (AJ), and a septate junction (SJ). (D-G) Confocal optical sections of wild type early stages egg chambers stained with antibodies against Mcr (D), Cont (E), Nrx-IV (F), and Cora (G) (Magenta and in individual channel in D'-G'), and co-stained with antibodies against Ecad (green) and labeled with DAPI. All four SJ proteins are expressed throughout the egg chamber along FC membranes, including SCs (arrowheads in D and E, and data not shown for Nrx-IV and Cora) and in the NCs. Mcr, Cont, and Nrx-IV (D-F) are found along the membrane and in puncta, whereas Cora is found predominantly at the membrane (G). In addition, Mcr, Cont, and Nrx-IV are highly expressed in the PCs (asterisks in D-F), whereas Cora is expressed in these cells with same level of expression relative to the FCs. Note that the focal plane of these images shows strong staining in PCs in only one side of the egg chamber, but Mcr, Cont and Nrx-IV are equally expressed in both anterior and posterior PCs. Anterior is to the left in each ovariole. Scale bar= 25μm.

Figure 2. Mcr, Cont, Nrx-IV, and Cora localization at later stages of oogenesis. (A) Diagram of a stage 12 egg chamber. (B-I) Confocal optical sections of wild type stage 11 – 12 egg chambers (B, D, F, and H) or stage 14 egg chamber (C, E, G, and I) stained with antibodies against Mcr (B and C), Cont (D and E), Nrx-IV (F and G), or Cora (H and I) (magenta and in individual channel in B', D', F', and H') and co-stained with antibodies against Ecad (green) and labeled with DAPI (blue). The location of these sections overlaps the boundary between the

oocyte (Oo.) and nurse cells (NCs) and is depicted as the red box in the diagram shown in (A). Note that Mcr, Cont, Nrx-IV, and Cora become enriched at the apical-lateral region of FCs membrane (arrows in B, D, F, and H). Insets show higher magnification of the indicated areas. The expression of all of these proteins persists in stage 14 egg chambers (C, E, G, and I). Anterior is to the left. Scale bar = 25μm in B, D, F, and H and 100μm in C, E, G, and I.

Figure 3. *SJ* genes are required for egg elongation. (A-G) Brightfield photomicrographs of stage 14 egg chambers. (A) *GR1-GAL4>UAS-GFP*, (B) *GR1-GAL4>UAS-Cont-RNAi*, (C) *GR1-GAL4>UAS-Nrx-IV-RNAi*, (D) *GR1-GAL4>UAS-Mcr-RNAi*, (E) *GR1-GAL4>UAS-cora-RNAi*, (F) *GR1-GAL4>UAS-sinu-RNAi*, and (G) *GR1-GAL4>UAS-Lac-RNAi*. Images in this figure represent average phenotypes observed in each genotype. (H and I) Quantification of length and width of stage 14 egg chambers from control and *SJ-RNAi* egg chambers. (J) Quantification of the aspect ratio of length (orange line in A) to width (yellow line in A) from control and *SJ-RNAi* stage 14 egg chambers. Note that the aspect ratio of all *SJ-RNAi* expressing egg chambers are statistically significant from the control egg chambers (unpaired T-test; $P<0.0001$). (K, L) Zoomed images of *GR1-GAL4>UAS-GFP* (K) and *GR1-GAL4>UAS-Lac-RNAi* (L) stage 14 egg chambers (from A and G) showing the dorsal appendages. The dorsal appendages in the *Lac-RNAi* egg chamber are either deformed or absent (arrows) compared to control dorsal appendages. (M) Quantification of dorsal appendage defects from control and *SJ-RNAi* stage 14 egg chambers. *n*, total number of egg chambers measured per genotype. Data represents individual values with mean ± s.d. *P* value <0.0001. Anterior is to the left. Scale bar = 100μm.

Figure 4. Mcr expression during border cell migration. (A) Diagram of border cell migration. At early stage 9 of oogenesis, a group of 4-6 follicle cells are specified by the polar cells (PCs) (green) to become border cells (BCs) (magenta). The BC/PC cluster delaminates apically and migrates between the nurse cells (NCs) until it reaches the oocyte (Oo.) by stage 10 of oogenesis. (B-D) Confocal optical images of wild type stage 9-10 egg chambers stained with antibodies against Mcr (magenta, and in ” panels), Fas3 (green, and in ”’ panels), and labeled with DAPI (blue, and in ”” panels). PCs are indicated with asterisks. Mcr is expressed in the PCs and BCs with higher expression at the interface between the PCs and BCs. Note that Mcr appears to be most enriched along the boundary with BCs at the leading edge of the border cell cluster (red arrows in B”-D”). Anterior is to the left. Scale bar = 25μm in (B-D) and 10μm in (B’-B’’’’ and D’-D’’’’).

Figure 5. Mcr, Cont, Nrx-IV, and Cora are required for effective border cell migration. (A-C) Border cell migration in control egg chambers. Egg chambers are immunostained with anti-Fas3 (magenta) to mark the polar cells, GFP (green) to mark border cells, and labeled with DAPI (blue). Arrows indicates border cell clusters. Note that in control egg chambers the border cell cluster reaches the oocyte at stage 10. (D-F) Stage 10 egg chambers expressing *Cont-RNAi* in border cells immunostained with anti-Cont (magenta) and anti-Fas3 (blue) showing examples of BC cluster migration defects: failed (arrow in D), incomplete (arrow in E), and disassociated border cell migration (arrow in F). Higher magnification of control (G) and *Cont-RNAi*-expressing (H) border cell clusters showing the dissociation of a border cell cluster observed in *SJ-RNAi* clusters. (I and J) Quantification of border cell cluster phenotypes at stage 10 egg

chambers in control and *SJ-RNAi* driven by either *Slbo-GAL4* (I) or *C306-GAL4* (J). Anterior is to the left. Scale bar = 25μm.

Figure 6. The apical-lateral localization of Cora depends on *Mcr*. (A-D) Confocal optical sections of stage 12 FCs stained with antibodies against Mcr (magenta, and in ' panels) and Cora (green, and in " panels) and labeled with DAPI (blue). Mcr and Cora co-localize at the presumptive SJ in control stage 12 egg chambers (A), whereas Mcr and Cora localize along the lateral membrane of *NrxIV-RNAi* expressing FCs (B). In most *Mcr-RNAi*-expressing stage 12 egg chambers, Cora localizes laterally (C), whereas in some egg chambers, Cora is enriched apically (D), but is often associated with Mcr puncta (arrows). Scale bar = 10μm.

Figure 7. Mcr and Cora require Rab5 and Rab11 for their correct localization at the SJ. (A-D) Confocal optical sections of stage 11 (A and B) or stage 12 (C and D) FCs stained with antibodies against Mcr (magenta, and in ' panels) and Cora (green, and in " panels) and labeled with DAPI (blue). While Mcr and Cora co-localize at the apical-lateral membrane of stage 11 and 12 control FCs (arrows in A and C), both Cora and Mcr fail to localize at the SJ in $Rab5^{DN}$-expressing FCs (B). In *Rab11-RNAi* expressing-FCs (D), Cora localizes along the lateral membrane, whereas Mcr is either missing (arrowhead) or localizes along the lateral membrane (arrow). Anterior is to the left. Scale bars = 10μm.

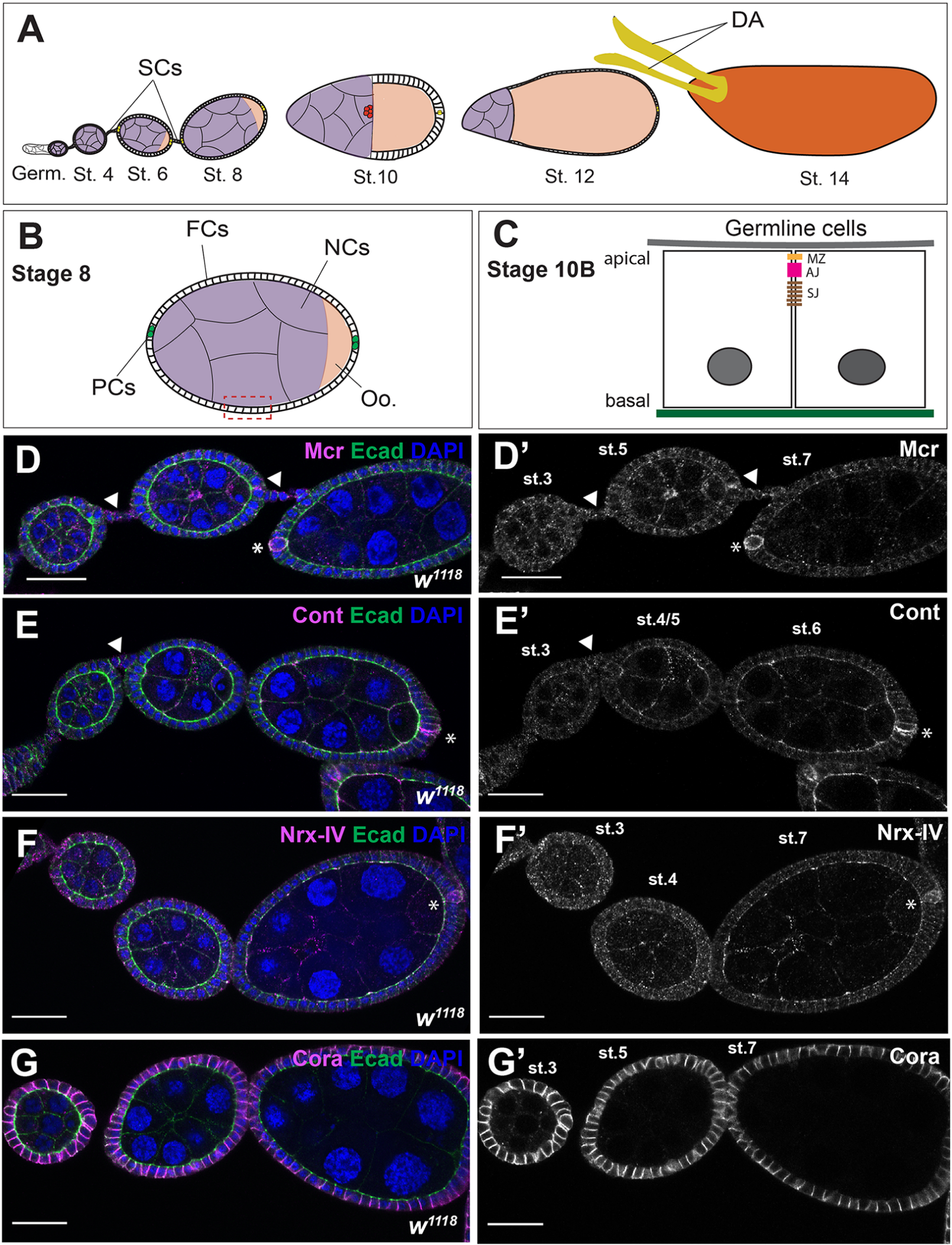
A
SCs
DA
Germ.
St. 4
St. 6
St. 8
St.10
St. 12
St. 14
B
Stage 8
FCs
NCs
PCs
Oo.
C
Stage 10B
Germline cells
apical
basal
MZ
AJ
SJ
D
Mcr Ecad DAPI
w1118
D'
st.3
st.5
st.7
Mcr
E
Cont Ecad DAPI
w1118
E'
st.3
st.4/5
st.6
Cont
F
Nrx-IV Ecad DAPI
w1118
F'
st.3
st.4
st.7
Nrx-IV
G
Cora Ecad DAPI
w1118
G'
st.3
st.5
st.7
Cora

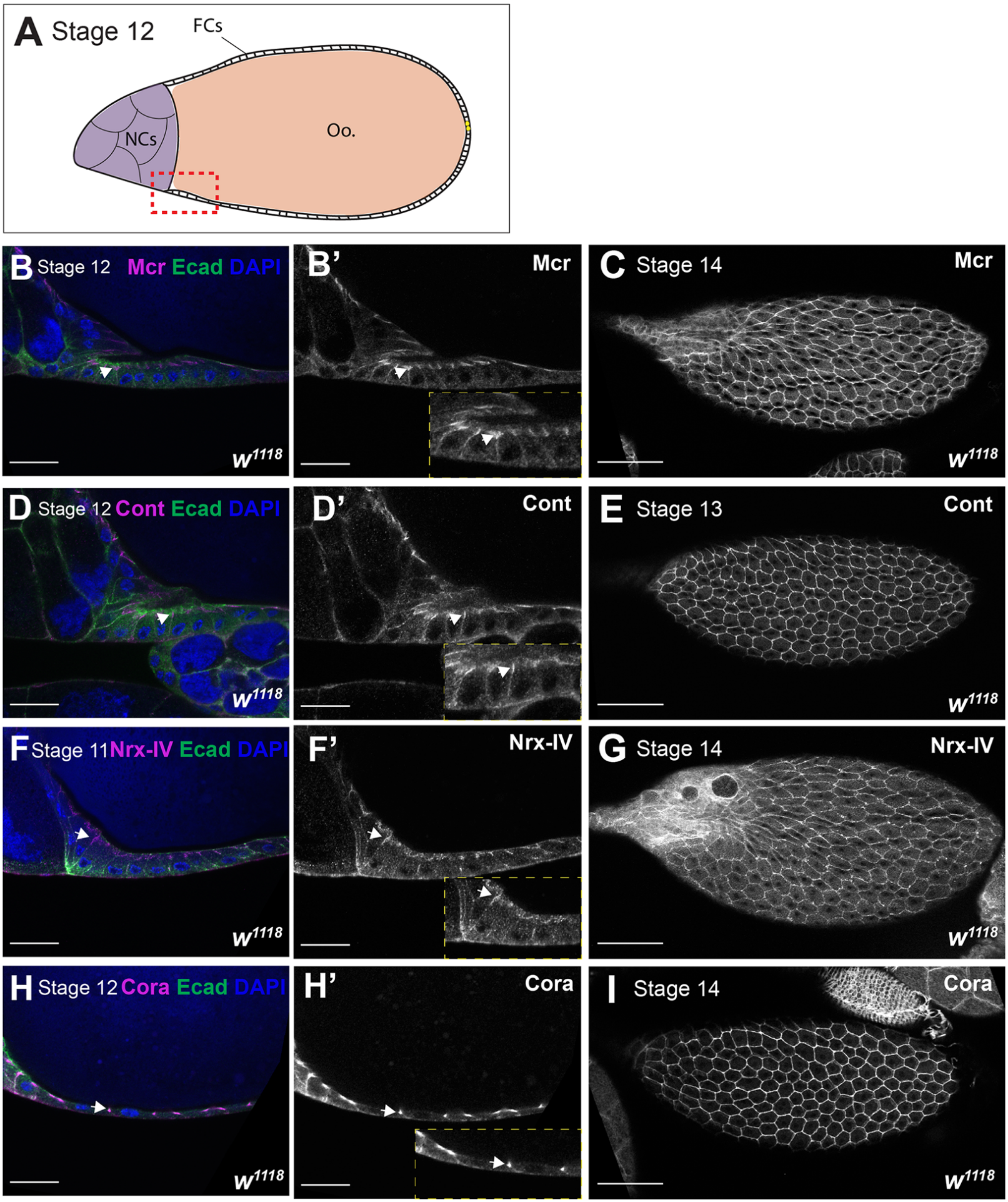
A Stage 12
FCs
NCs
Oo.
B Stage 12 Mcr Ecad DAPI
w1118
B' Mcr
C Stage 14 Mcr
w1118
D Stage 12 Cont Ecad DAPI
w1118
D' Cont
E Stage 13 Cont
w1118
F Stage 11 Nrx-IV Ecad DAPI
w1118
F' Nrx-IV
G Stage 14 Nrx-IV
w1118
H Stage 12 Cora Ecad DAPI
w1118
H' Cora
I Stage 14 Cora
w1118

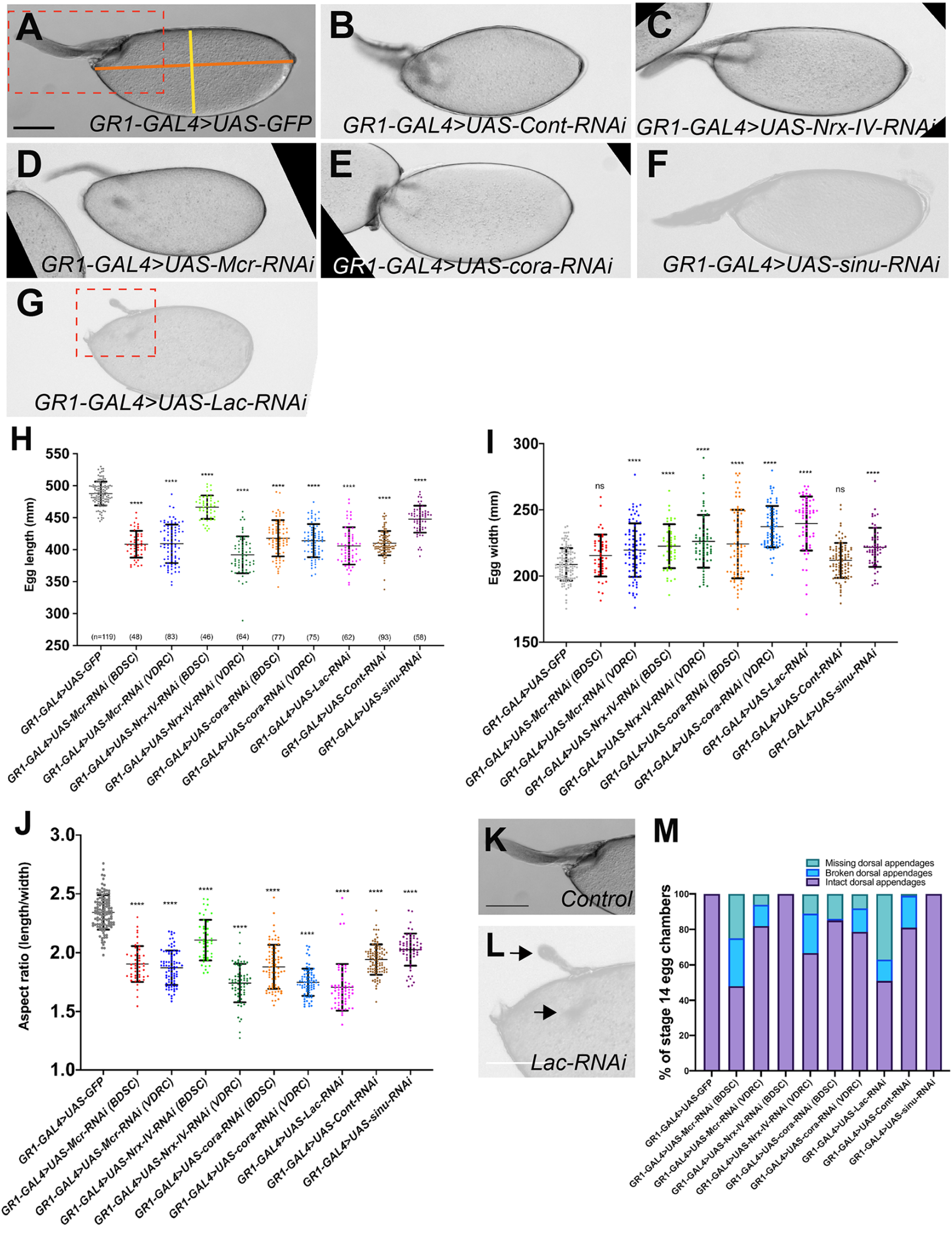
A
GR1-GAL4>UAS-GFP
B
GR1-GAL4>UAS-Cont-RNAi
C
GR1-GAL4>UAS-Nrx-IV-RNAi
D
GR1-GAL4>UAS-Mcr-RNAi
E
GR1-GAL4>UAS-cora-RNAi
F
GR1-GAL4>UAS-sinu-RNAi
G
GR1-GAL4>UAS-Lac-RNAi
H
Egg length (mm)
550
500
450
400
350
300
250
(n=119)
(48)
(83)
(46)
(64)
(77)
(75)
(62)
(93)
(58)
****
GR1-GAL4>UAS-GFP
GR1-GAL4>UAS-Mcr-RNAi (BDSC)
GR1-GAL4>UAS-Mcr-RNAi (VDRC)
GR1-GAL4>UAS-Nrx-IV-RNAi (BDSC)
GR1-GAL4>UAS-Nrx-IV-RNAi (VDRC)
GR1-GAL4>UAS-cora-RNAi (BDSC)
GR1-GAL4>UAS-cora-RNAi (VDRC)
GR1-GAL4>UAS-Lac-RNAi
GR1-GAL4>UAS-Cont-RNAi
GR1-GAL4>UAS-sinu-RNAi
I
Egg width (mm)
300
250
200
150
ns
****
J
Aspect ratio (length/width)
3.0
2.5
2.0
1.5
1.0
K
Control
L
Lac-RNAi
M
% of stage 14 egg chambers
100
80
60
40
20
0
Missing dorsal appendages
Broken dorsal appendages
Intact dorsal appendages

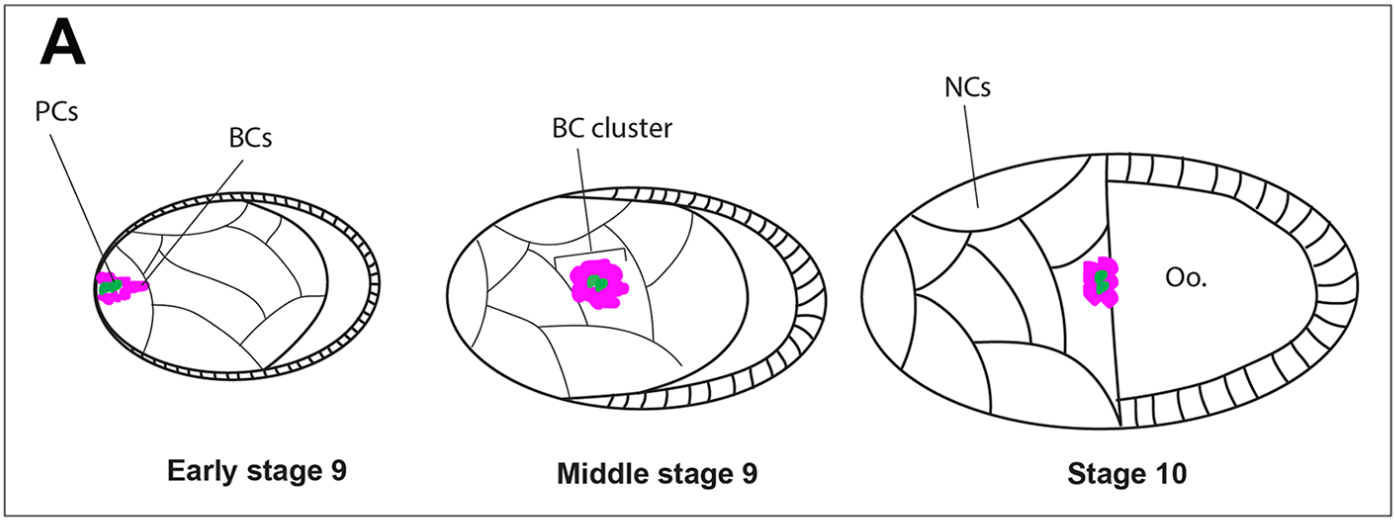
A
PCs
BCs
BC cluster
NCs
Oo.
Early stage 9
Middle stage 9
Stage 10

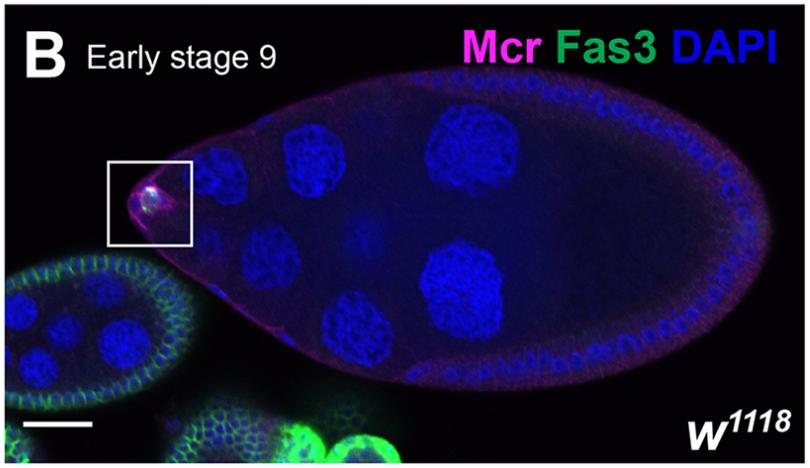
B Early stage 9
Mcr Fas3 DAPI
w1118

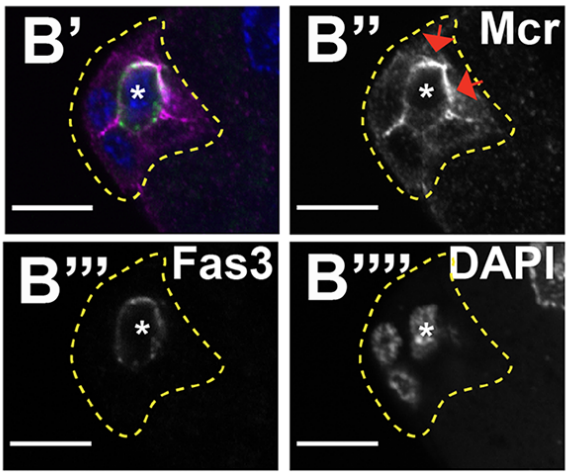
B'
B''
Mcr
B'''
Fas3
B''''
DAPI

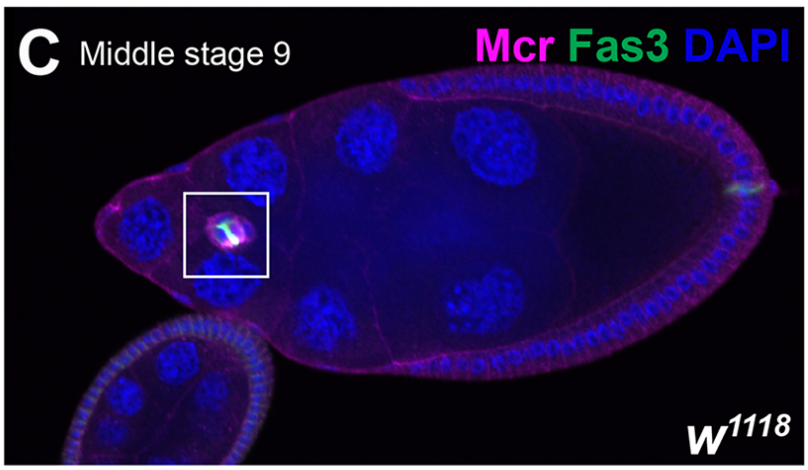
C Middle stage 9
Mcr Fas3 DAPI
w1118

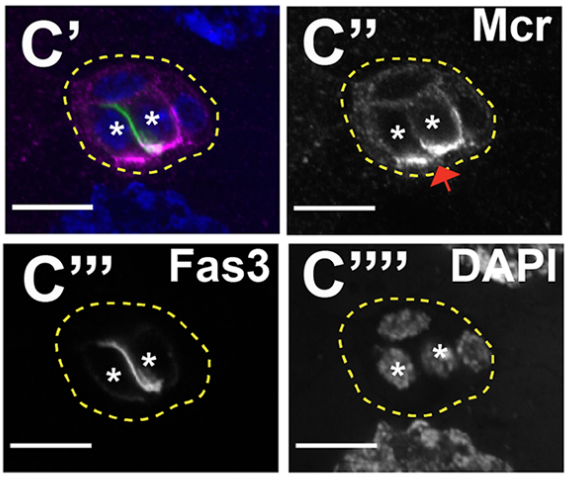
C'
C''
Mcr
C'''
Fas3
C''''
DAPI

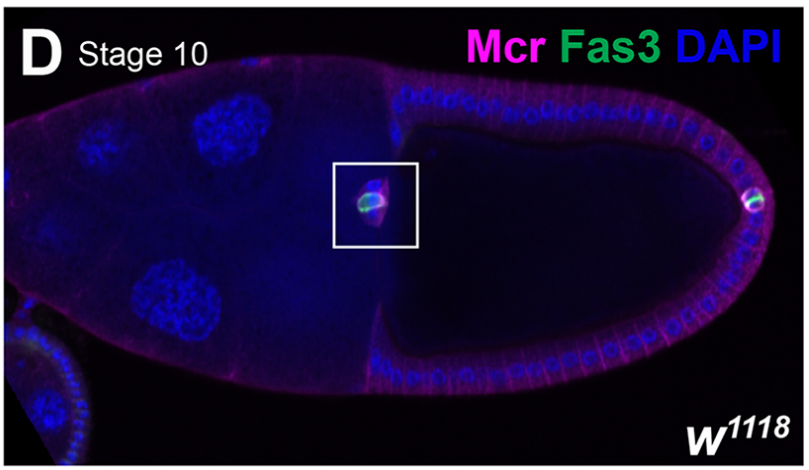
D Stage 10
Mcr Fas3 DAPI
w1118

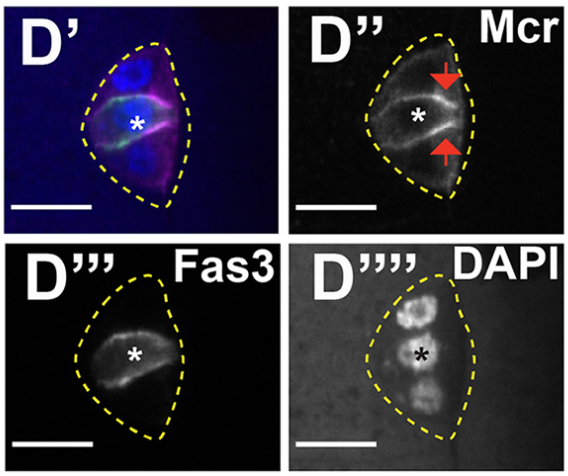
D'
D''
Mcr
D'''
Fas3
D''''
DAPI

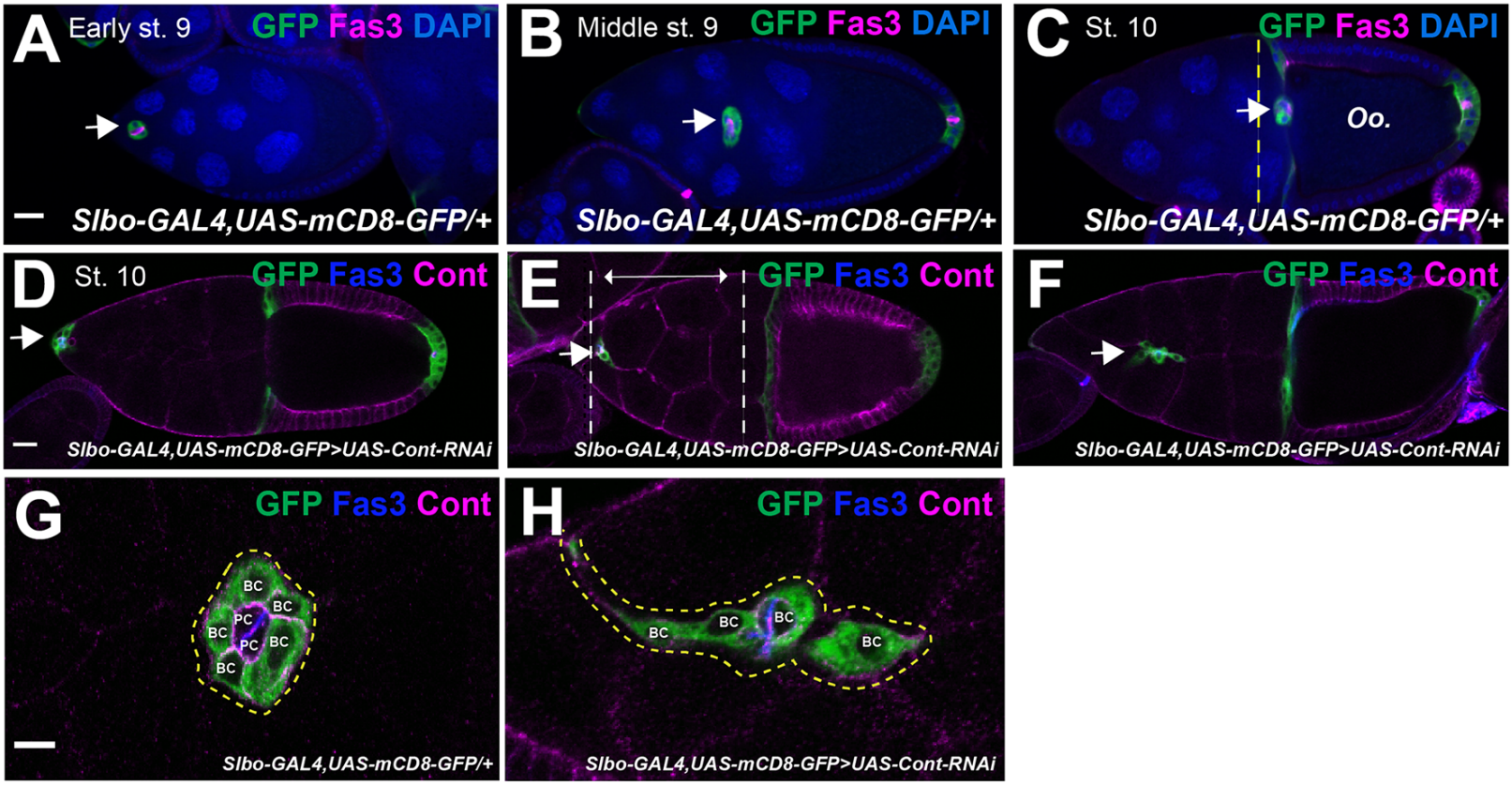
A
Early st. 9
GFP Fas3 DAPI
Slbo-GAL4,UAS-mCD8-GFP/+
B
Middle st. 9
GFP Fas3 DAPI
Slbo-GAL4,UAS-mCD8-GFP/+
C
St. 10
GFP Fas3 DAPI
Oo.
Slbo-GAL4,UAS-mCD8-GFP/+
D
St. 10
GFP Fas3 Cont
Slbo-GAL4,UAS-mCD8-GFP>UAS-Cont-RNAi
E
GFP Fas3 Cont
Slbo-GAL4,UAS-mCD8-GFP>UAS-Cont-RNAi
F
GFP Fas3 Cont
Slbo-GAL4,UAS-mCD8-GFP>UAS-Cont-RNAi
G
GFP Fas3 Cont
BC
PC
Slbo-GAL4,UAS-mCD8-GFP/+
H
GFP Fas3 Cont
BC
Slbo-GAL4,UAS-mCD8-GFP>UAS-Cont-RNAi

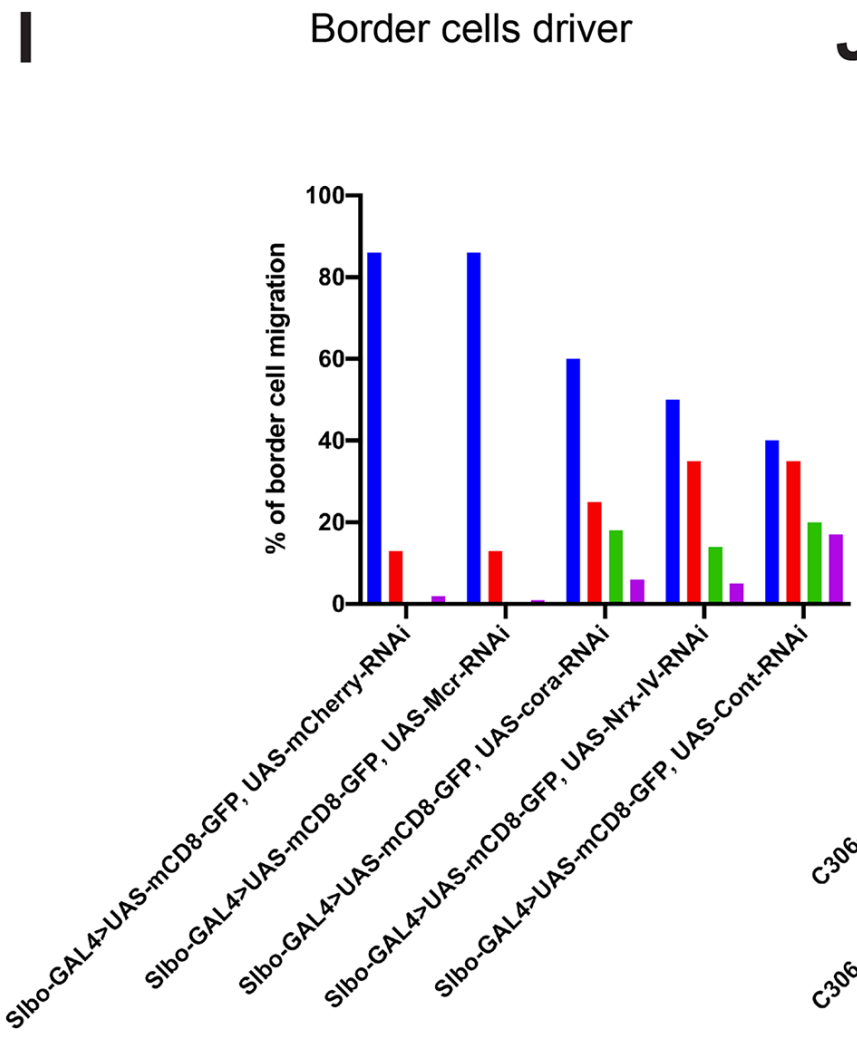
I
Border cells driver
% of border cell migration
100
80
60
40
20
0
Slbo-GAL4>UAS-mCD8-GFP, UAS-mCherry-RNAi
Slbo-GAL4>UAS-mCD8-GFP, UAS-Mcr-RNAi
Slbo-GAL4>UAS-mCD8-GFP, UAS-cora-RNAi
Slbo-GAL4>UAS-mCD8-GFP, UAS-Nrx-IV-RNAi
Slbo-GAL4>UAS-mCD8-GFP, UAS-Cont-RNAi

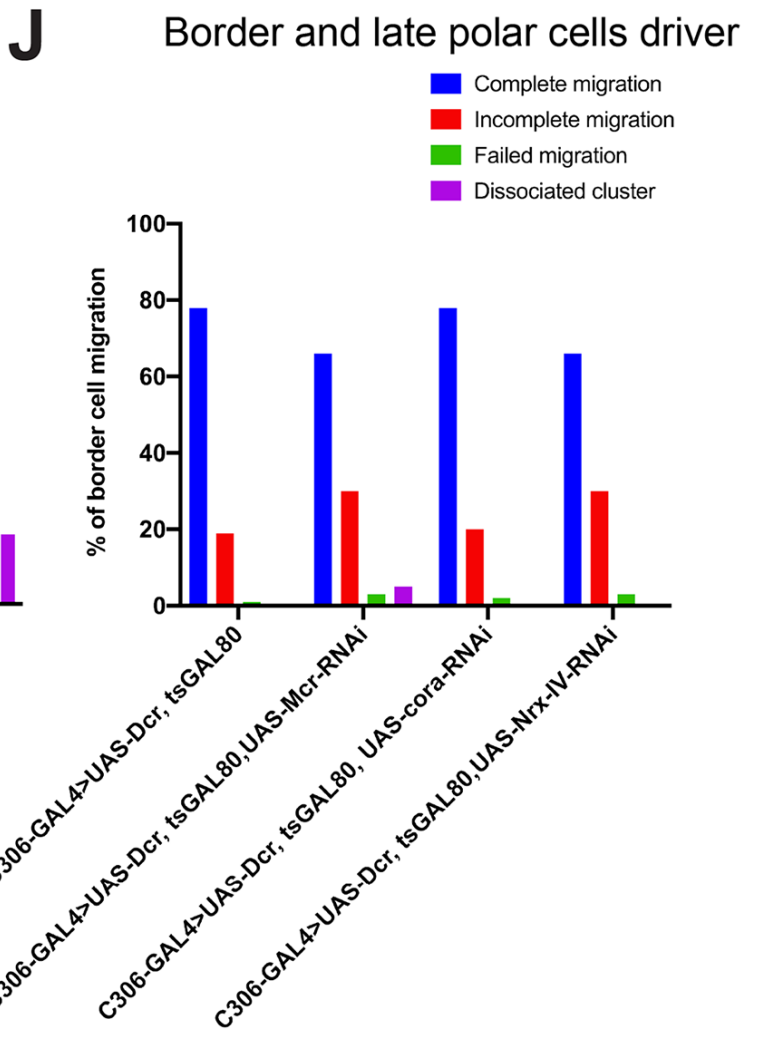
J
Border and late polar cells driver
Complete migration
Incomplete migration
Failed migration
Dissociated cluster
% of border cell migration
100
80
60
40
20
0
C306-GAL4>UAS-Dcr, tsGAL80
C306-GAL4>UAS-Dcr, tsGAL80,UAS-Mcr-RNAi
C306-GAL4>UAS-Dcr, tsGAL80, UAS-cora-RNAi
C306-GAL4>UAS-Dcr, tsGAL80,UAS-Nrx-IV-RNAi

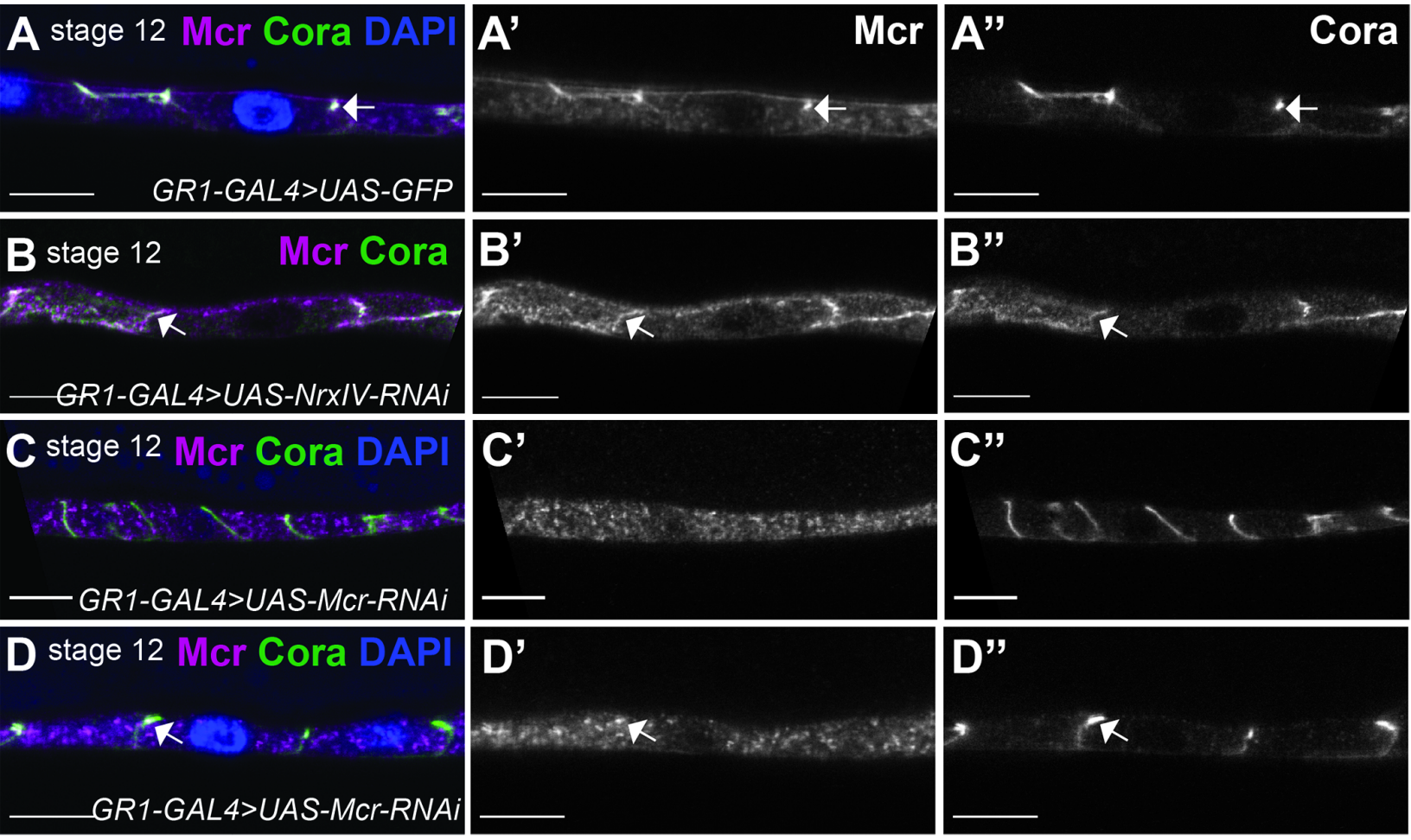
A stage 12 Mcr Cora DAPI
GR1-GAL4>UAS-GFP
A' Mcr
A'' Cora
B stage 12 Mcr Cora
GR1-GAL4>UAS-NrxIV-RNAi
B'
B''
C stage 12 Mcr Cora DAPI
GR1-GAL4>UAS-Mcr-RNAi
C'
C''
D stage 12 Mcr Cora DAPI
GR1-GAL4>UAS-Mcr-RNAi
D'
D''

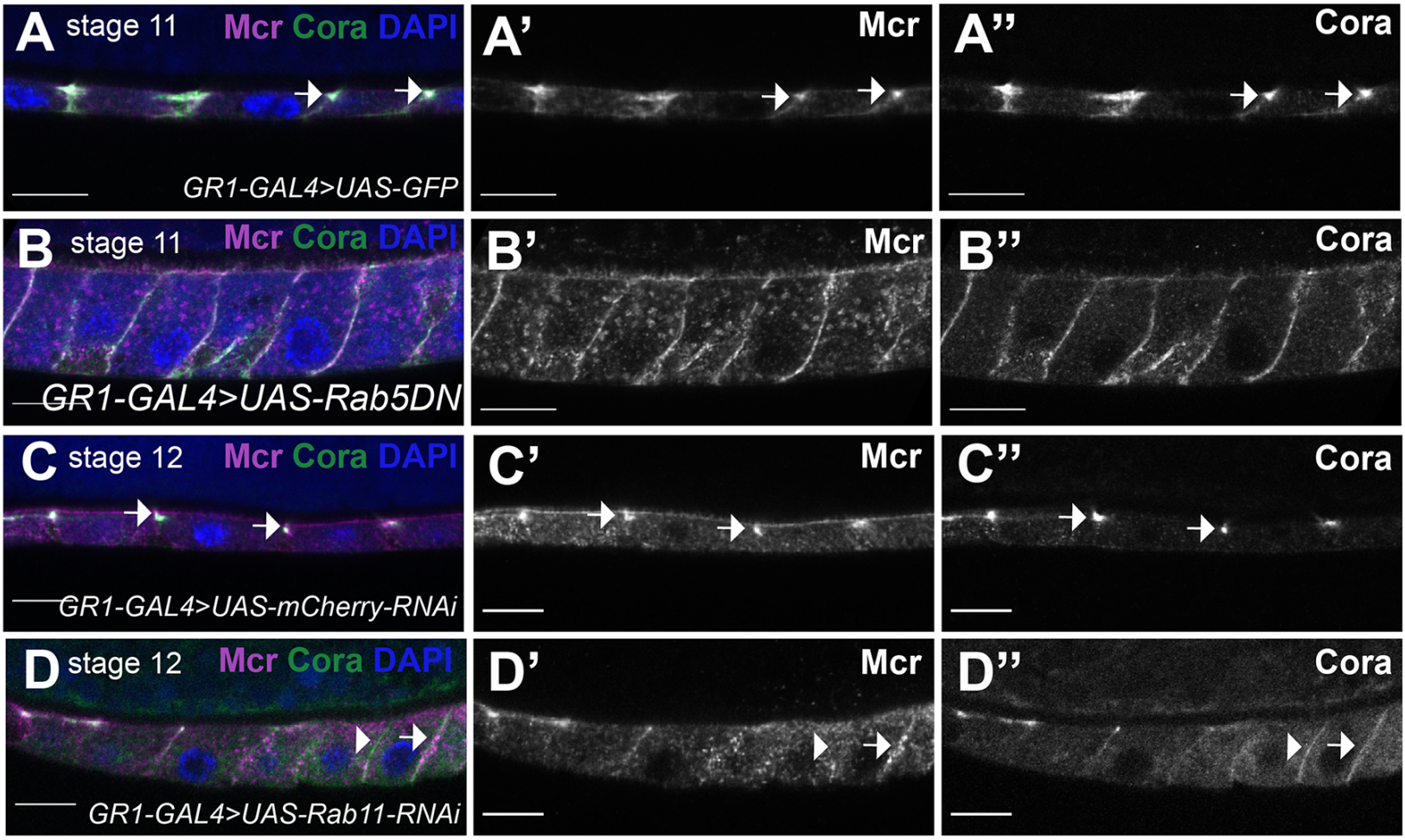
A stage 11 Mcr Cora DAPI
GR1-GAL4>UAS-GFP
A' Mcr
A'' Cora
B stage 11 Mcr Cora DAPI
GR1-GAL4>UAS-Rab5DN
B' Mcr
B'' Cora
C stage 12 Mcr Cora DAPI
GR1-GAL4>UAS-mCherry-RNAi
C' Mcr
C'' Cora
D stage 12 Mcr Cora DAPI
GR1-GAL4>UAS-Rab11-RNAi
D' Mcr
D'' Cora